

Resource Management in Quantum Virtual Private Networks

Shahrooz Pouryousef*, Nitish K. Panigrahy*, Monimoy Deb Purkayastha†, Sabyasachi Mukhopadhyay†, Gert Grammel†, Dominoko Di Mola† and Don Towsley *

*University of Massachusetts Amherst. †Juniper Networks.

Email: *{shahrooz,nitish,towsley}@cs.umass.edu, † {monimoy,sabyas,ggrammel,domenico}@juniper.net

Abstract—In this study, we develop a resource management framework for a *quantum virtual private network* (qVPN), which involves the sharing of an underlying public quantum network by multiple organizations for quantum entanglement distribution. Our approach involves resolving the issue of link entanglement resource allocation in a qVPN by utilizing a centralized optimization framework. We provide insights into the potential of genetic and learning-based algorithms for optimizing qVPNs, and emphasize the significance of path selection and distillation in enabling efficient and reliable quantum communication in multi-organizational settings. Our findings demonstrate that compared to traditional greedy based heuristics, genetic and learning-based algorithms can identify better paths. Furthermore, these algorithms can effectively identify good distillation strategies to mitigate potential noises in gates and quantum channels, while ensuring the necessary quality of service for end users.

I. INTRODUCTION

The advent of a quantum network will unlock unprecedented possibilities for novel applications, including quantum key distribution [2], [23], [31], [28], distributed quantum computation [7], quantum sensing [9], and clock synchronisation [18]. Crucial to the realization of these applications is the ability to distribute quantum entanglements across long distances. Therefore, the primary responsibility of the first and second generation quantum networks [20] will be to facilitate the delivery of bipartite quantum entanglements, also known as EPR pairs, to distinct pairs of end-users.

These end-users may belong to various organizations, requiring entanglement distribution service among members belonging to the same organization. Creating individual private quantum networks with dedicated quantum links and switches for each organization may not be scalable due to high infrastructure and operational costs. Thus there exists a critical need for the development of a *quantum virtual private network* (qVPN) architecture that enables multiple organizations to share an underlying public quantum network, analogous to the classical VPNs [13], [11].

In this work, we lay out the foundations of a qVPN architecture. Imagine that a group of private organizations need to create intra-organizational EPR pairs between end-users on their sites located in different geographical locations. Figure 1 shows the schematic of such an architecture where an underlying public quantum network is shared among the three organizations. Each organizational site may have an ingress

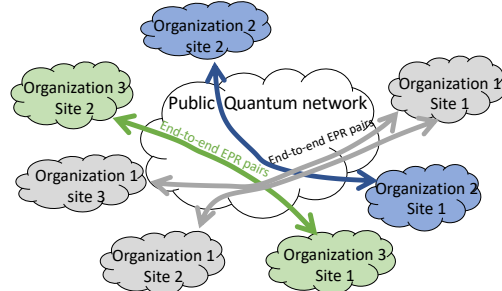


Figure 1: A quantum network shared by multiple organizations

node (i-node) and an egress node (e-node). The responsibility of the public quantum network would be to distribute EPR pairs between the i-nodes and e-nodes of different sites (i-e EPRs), while the organizations themselves would need to create EPR pairs within their respective sites (site EPRs) between end-users and i/e-nodes. Finally, entanglement swap operations would be performed between the site EPRs and i-e EPRs to create end-to-end EPR pairs (E2E EPRs) between users.

Establishing a shared quantum network entails resolving a set of fundamental optimization challenges. For example, the E2E EPRs may be consumed by independent applications executed by end-users, enforcing a minimum required value of rate and quality for the generated entanglements. Entanglement generation procedure in a quantum network is inherently lossy and noisy. Thus, to ensure the quality of service requirements, one needs to appropriately allocate the limited underlying quantum network resources to different organizations. Further, organizations may prioritize their members differently when it comes to establishing entanglement. Moreover, the relative importance assigned to each organization in the optimization process may potentially influence entanglement routing, and network resource allocation decisions within the shared public network. One of the goals of this work is to address these challenges to ensure efficient and reliable operation of a qVPN.

In order to optimize the performance of a qVPN, it is also necessary to identify several entanglement generating paths that connect a particular pair of end-users. However, in many cases, there can be an exponential number of simple paths connecting any two nodes in the public network, making it

difficult to consider all possible paths for large networks. In addition, different amounts of entanglement distillation¹ at different places of the network may be required to preserve the fidelity requirements of various organizations and their user pairs. As a result, it becomes crucial to use efficient heuristics to select the most optimal paths and distillation strategies. In this work, we use two heuristic based algorithms: (i) an evolutionary derivative-free Genetic Algorithm (GA), and (ii) a Gradient-based Deep Reinforcement learning (GDR) algorithm for selecting paths and distillation strategies.

Once a set of paths is selected for every pair of end-users, we tackle an optimization problem aimed at maximizing the total weighted entanglement generation rate (WEGR) for all pairs of end-users across different organizations where different end-user pairs can have different weights, while adhering to link capacity and QoS constraints. Although maximizing WEGR is important, ensuring a fair distribution of rates among end-user pairs prevents any single user or application from monopolizing the available resources. To attain this goal, we introduce constraints on the maximum number of E2E EPR pairs that can be served to each pair of end-users.

Our contributions are summarized below.

- We introduce a quantum virtual private network (qVPN) architecture designed to optimize the distribution of quantum entanglements in a multiorganization setting. To the best of our knowledge, this is the first study to provide a comprehensive design and performance analysis of a qVPN.
- We present an optimization framework for a qVPN to maximize the aggregate weighted entanglement generation rate, subject to link capacity and QoS constraints.
- We evaluate the effectiveness of our proposed architecture through extensive numerical simulations. Our results confirm that GA and learning based solution provide 20 – 30% improvement in W-EGR over the state-of-the-art baselines.

The rest of the paper is organized as follows. First, we define the resource allocation problem in qVPN in Section II. In Section III, we explain two path and distillation selection heuristics of our proposed qVPN architecture. An in-depth assessment of the suggested framework’s performance is carried out in Section IV. We list the related work in Section V and conclude the paper in Section VI.

II. RESOURCE ALLOCATION IN QVPN

We represent the network as a graph $G(V, E)$ shared by a set of organizations \mathcal{K} where V is the set of nodes and E the set of links. Link $l \in E$ generates entanglements (link-level EPRs) with fidelity F_l at rate c_l . Each organization k has a set of user pairs U_k that are connected by one or more paths. We associate a weight w_k with organization $k \in \mathcal{K}$ and each user pair u in organization k has a weight indicated by λ_u^k . We assume

¹Entanglement distillation is a quantum operation that can be performed on low quality EPRs to generate fewer number of high quality EPRs that achieve a target fidelity.

$G(V, E)$	Graph with set of nodes V and set of links E
c_l	Capacity of link $l \in E$ in EPRs/sec
\mathcal{K}	Set of K organizations
$U_k \subset V \times V$	set of user pairs in organization $k \in \mathcal{K}$
w_k	Weight of organization $k \in \mathcal{K}$
λ_u^k	Weight of user pair $u \in U_k$ in organization $k \in \mathcal{K}$
P_u^k	Set of paths connecting user pair u from organization k
F_u^k	Fidelity threshold of user pair u from organization $k \in \mathcal{K}$
$g_p(F_l, F_u^k)$	Avg. no. of link-level EPR pairs needed for distillation on path p to achieve fidelity threshold F_u^k
q	Swap success probability
$x_{u,p}^k$	Entanglement generation rate for user pair u in organization $k \in \mathcal{K}$ on path p

Table I: Notations used in formulation.

each user pair u has a requirement for maintaining a certain fidelity threshold for the EPR pairs that are provided to them. We represent this fidelity threshold as F_u^k . We assume a static fidelity model, meaning that the fidelities of link-level and end-to-end EPRs degrade when entanglement swap, entanglement distillation, measurement, and gate operations are carried out. The notations used in this paper are found in Table I.

We formulate the resource allocation problem as maximizing the aggregate weighted Entanglement Generation Rate (W-EGR) with respect to satisfying all user pair fidelities F_u^k . There are minimum and maximum rate constraints, $R_{min}^{k,u}$ and $R_{max}^{k,u}$ associated with each user pair. Our assumption is that every pair of users u , belonging to each organization k , has access to a set of one or more paths², denoted as P_u^k .

To satisfy the fidelity threshold requirement of each user, it may be necessary to perform entanglement distillation on each path. Distillation on a path can be performed at two different levels: link-level and end-to-end. In link-level distillation, the fidelities of individual link-level EPRs on a path are enhanced at the expense of some link capacity. Further, the quality of the E2E EPRs can be improved via end-to-end distillation. We employ both link-level and end-to-end distillation in our approach. Let $g_p(F_l, F_u^k)$ represent the average number of link-level EPRs required for distillation on link l having fidelity F_l to achieve a minimum E2E fidelity of F_u^k , for user u over path $p \in P_u^k$. This function, $g_p(F_l, F_u^k)$, can be computed for various distillation approaches [10], and we will provide further details on this matter in Section § III-C. We now formulate the following weighted EGR maximization problem for a qVPN.

²Using Entanglement Swapping, it is possible to establish an E2E EPR between a pair of users u by utilizing one link-level EPR pair for each link present on the path connecting users u .

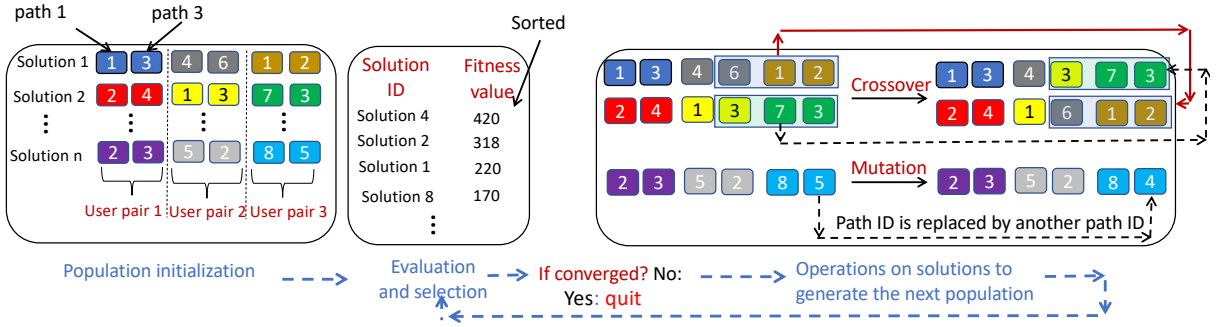


Figure 2: A flowchart illustrating the genetic algorithm process for path selection.

$$\max_{x_{u,p}^k} \sum_{k \in \mathcal{K}} \sum_{u \in U_k} \sum_{p \in P_u^k} w_k x_{u,p}^k \lambda_u^k q^{|p|-1} \quad (1)$$

s.t.

$$\sum_{\substack{k \in \mathcal{K} \\ u \in U_k \\ p \in P_u^k | l \in p}} x_{u,p}^k g_p(F_l, F_u^k) \leq c_l, \quad l \in E \quad (2)$$

$$\sum_{p \in P_u^k} x_{u,p}^k \geq R_{min}^{k,u} \quad k \in \mathcal{K}, u \in U_k \quad (3)$$

$$\sum_{p \in P_u^k} x_{u,p}^k \leq R_{max}^{k,u} \quad k \in \mathcal{K}, u \in U_k \quad (4)$$

$$x_{u,p}^k \geq 0, \quad k \in \mathcal{K}, u \in U_k, p \in P_u^k \quad (5)$$

The decision variables in our optimization problem in (1) are $\{x_{u,p}^k\}$ where for each path p , $x_{u,p}^k$ denotes the entanglement generation rate for user pair u from the organization $k \in \mathcal{K}$ on path p and q is the swap success probability. Here (2) represents the link capacity constraints, and (3) and (4) represent the minimum and maximum rate constraints for each user pair.

The optimization problem presented in (1) assumes that both the set of paths and the corresponding distillation strategy are already known. We will elaborate on our approach for selecting network paths and the associated distillation strategies in the following section.

III. PATH SELECTION AND DISTILLATION IN QVPN

This section outlines two methods for selecting paths in a qVPN, as well as determining effective distillation strategies for each path to minimize distillation resource expenditure. The selection of a path and corresponding distillation strategy is based on the path's end-to-end fidelity and the required fidelity threshold of the user pair utilizing that path, along with other constraints such as minimum and maximum rate constraints for user pairs. Since it is impractical to compute all possible paths for all user pairs in various organizations and test every possible distillation strategy, we propose the following two distinct schemes. We describe an evolutionary derivative-free approach (via genetic algorithm), as well as a

gradient-based approach (via gradient-based deep reinforcement learning) for selecting paths and distillation strategies in a qVPN.

A. Genetic algorithm for path selection

The Genetic Algorithm (GA) is a heuristic-based approach for solving optimization problems. Initially, GA starts with a population of candidate solutions randomly chosen from the search space of the problem. These candidate solutions undergo successive iterations and a new generation is evolved as a result. Figure 2 shows how we formulate a candidate solution in our context.

In our GA approach, a candidate solution is represented as a list with assigned ranges of indices for each user pair. Figure 2 illustrates this concept, where the first two values of the list correspond to the path IDs for the first user pair. We assume that each user pair can use at most two paths in the network, and the path IDs shown in the figure are randomly selected from a larger set of paths called *candidate paths*. These candidate paths are created for each user pair using heuristic schemes like shortest paths, which we elaborate on in Section §IV.

Once the initial population is created, each candidate solution is assessed and assigned a fitness value, which indicates its quality. In our approach, the fitness value for each candidate solution is the W-EGR obtained by solving optimization problem 1 using the set of paths in that candidate solution as an input. There are three primary operations in a GA: Selection, Crossover and Mutation. To generate new candidate solutions, we apply these operations to each existing candidate solution as follows.

In Figure 2, the GA operates on a set of n candidate solutions. Candidate solutions 1 and 2 are first selected for the crossover operation. As shown, the first three cells of candidate solution 1 are moved directly to the first (top) new candidate solution in the next generation, and the second half of candidate solution 2 is moved to the second part of the first new candidate solution. For the mutation operation, the last cell in candidate solution n is selected. Subsequently, the GA evaluates the fitness values of the new population.

1) *Exploration vs. exploitation in GA*: GA applies mutation and crossover operations to create new candidate solutions. In

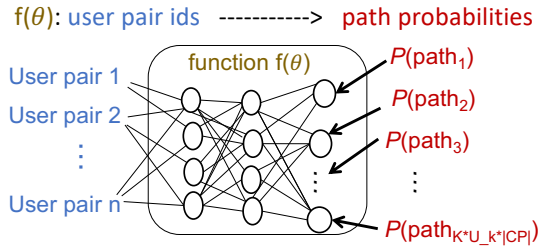


Figure 3: Representing the function of path selection as a neural network.

the *dynamic version* of GA, the algorithm adapts its policy for these operations over time to balance exploration of the search space with exploitation of what has been discovered so far. More specifically, the dynamic version of GA tends to explore the search space more in the early generations and reduces exploration as time passes. This is controlled by adjusting the probability of mutation and crossover and the selection operation. For example, the dynamic GA may give most of the candidate solutions in the early generations a chance to generate the next population, while using higher values for the probability of mutation and crossover. In contrast, the static version of GA always uses the same strategy for selection, such as using a fixed subset of candidate solutions to generate the next population. We assess the effectiveness of both static and dynamic approaches via numerical simulations in Section IV.

B. Gradient-based reinforcement learning for path selection

We now employ a neural network as a policy function, which can be adjusted to map the given set of user pairs to a probability distribution representing the likelihood of selecting each path for every user pair. Unlike genetic algorithms (GA), this method is based on derivatives and we formulate the learning aspect of this approach as a reinforcement learning problem.

Figure 3 depicts how a neural network is used to learn a set of paths for our optimization problem. Path selection is obtained by training the neural network, where the input is a list of user pairs and the output is the probability of selecting each path in the network. If there are K organizations and U_k user pairs in each organization, and $|CP|$ candidate paths for each user pair, the output size of the neural network is $KU_k|CP|$. From this output, we select R paths, where R is equal to $KU_k|P|$, and $|P|$ is the maximum number of paths allowed to be used by each user pair ($|P| \leq |CP|$). We select the paths with the largest probabilities as inputs to problem (1) and calculate the aggregate weighted EGR. We then use the computed W-EGR to update the weights of our neural network and improve the neural network model. We repeat this process to derive a function policy that maps the set of user pairs to an output indicating the paths that maximize the aggregate W-EGR. Further details about the training algorithm are provided in Appendix VII, Algorithm §1.

C. Distillation strategies

A distillation strategy for a path involves determining the appropriate amount of link-level and end-to-end distillation necessary to attain the desired E2E fidelity level. For example: consider a path p used to create E2E EPR pair between user pair u for organization k . For a path with a length of N and identical link fidelities set to F_L , the resulting fidelity of the E2E EPR pair between u after undergoing N nested swap operations can be expressed as

$$S(F_L) = \frac{1}{4} + \frac{3}{4} \left(\frac{P_2(4\eta^2 - 1)}{3} \right)^{N-1} \left(\frac{4F_L - 1}{3} \right)^N \quad (6)$$

where P_2 is the two-qubit gate fidelity and η is the measurement fidelity of the swapping operation. Let $F_{out} = \hat{S}(F_{in})$ represent the relationship between input and output fidelities of a distillation algorithm. A distillation strategy for path p can then be defined as a fidelity threshold for link-level EPRs (say $F_L^{th} > F_L$) such that $\hat{S}(S(F_L^{th})) \geq F_u^k$. The format of the candidate solution (or output) in GA (or Gradient-based RL) in Section III-A (or III-B) can be modified to include both p and F_L^{th} for joint path and distillation strategy selection.

IV. EVALUATION

In this section, we conduct a comprehensive set of experiments aimed at assessing various approaches for selecting path and distillation strategies in a qVPN. We have chosen three different baselines based on the shortest paths between user pairs. These schemes use the shortest paths in the network for each user pair when the link weights in the network are set to one (for Shortest hop-based scheme), to $1/\text{EGR}$ (for Shortest EGR-based scheme) and $1/\text{EGR}^2$ (for Shortest EGR-Square-based scheme) with EGR being the link capacity. For each user pair in each organization, we compute the set of candidate paths for GA and Gradient-based scheme using the k -shortest path algorithm proposed in [32] with $k = 5$. Our goal is to address the following research questions: (1) How do the performance of GA and the *Gradient-based* scheme compare to that of the alternative greedy baseline methods? (2) How do search space and problem size affect the convergence of GA and the gradient-based scheme? (3) Can GA effectively identify suitable distillation strategies for various paths and different fidelity thresholds in order to mitigate noisy gates and meet user requirements? (4) How can we ensure fair resource allocation in a qVPN?

Network topology: In our evaluation, we use the Dutch SURFnet network, taken from the Internet topology zoo [21]. We obtain the geographical location of the nodes in this network from the zoo topology data set [21] and compute the length of each link accordingly.

Computing link capacities: We assume link-level EPR pairs are generated using a single-photon scheme [14]. In addition, we assume one can control the rate and the fidelity of the generated EPR pairs on each link with a tunable parameter α [14]. In other words, we assume that each LLE is modelled by a state of the form $\rho = (1 - \alpha)|\Psi\rangle\langle\Psi^+| + \alpha|\uparrow\uparrow\rangle\langle\uparrow\uparrow|$

Param	\mathcal{K}	w_k	λ_u^k	F_u^k
Value	3	Unif[0.1, 1.0]	Unif[0.3, 0.7]	Unif[0.75, 0.90]

Table II: Parameters used in our experiments.

with probability $p = 2\eta_l\alpha$ where η_l is the transmissivity for link l with length d_l . η_l is computed as $\eta_l = 10^{-0.1\beta d_l}$ with $\beta = 0.2$ dB/km and is the fiber attenuation coefficient. Then, we compute the rate as $\frac{p}{T}$ where T is the repetition time. We set T to one μs and α to 0.2 in our experiments, resulting in the link fidelities being configured to 0.8.

Engineering the SURFnet topology: Some of the longer links in the SURFnet topology produce significantly lower EPR rates compared to other shorter links. For this reason, we engineer this topology by adding a repeater every 10km along links exceeding 20km in length. However, we do not allow these newly added repeater nodes to be used as end points for users. Additionally, we assume a multiplexing factor of three for each link, effectively tripling its capacity.

Purification protocol: In our experiments, we use the recurrence-based purification scheme [12]. In particular, we use the DEJMPS protocol [10] for purification. The values of the function $g(\cdot)$ for different initial fidelity and target fidelity thresholds can be determined from the results presented in [10]. In our experiments, we assume $P_2 = 1$ and $\eta = 0.99$.

Workloads We assume there are three organizations in a qVPN and each organization has 50 user pairs unless noted otherwise. We randomly select the user pairs in the network among the nodes of the original SURFnet topology and set their fidelity threshold uniformly from the interval of [0.75, 0.90]. We select nodes whose shortest hop-based path length is no more than 7. Table II shows the value of different parameters used in our experiments. In Figures 4a, 4b, 4c, and Figure 5 we assume $R_{min}^{k,u} = 10$ for all user pairs in each organization and $R_{max}^{k,u} = 1,000$ unless otherwise specified. We consider four distinct workloads and plot the results of GA as the average of two runs for each of them. Each workload indicates 50 user pairs for three different organizations with varying fidelity thresholds and user pair weights.

In all our experiments, we solve optimization problem 1 using the IBM CPLEX solver [15].

Distillation strategies: We consider 16 distillation strategies for each path in our experiment. These strategies are constructed by selecting the link-level fidelity thresholds from a fixed set of fidelities ranging between 0.8 and 0.998. We use a link-level fidelity threshold of 0.992 for the greedy-based heuristic schemes.

Implementation: We develop our GA algorithm in Python and the gradient-based scheme in Python and TensorFlow [1] framework. For the gradient-based scheme, our policy neural network has three layers. The first layer is a convolutional layer with 128 filters. The kernel size is 33 and the stride is set to 1. The second layer is a fully-connected layer with 128 neurons. We use Leaky ReLU for the activation function for the first two layers. The final layer is a fully connected

linear layer (without activation function) with $N * (N - 1)$ neurons corresponding to all possible sets of user pairs in the network. The softmax function is applied to the output of the final layer to generate the probabilities for all available actions. The learning rate is initially configured to 0.0001 and decays every 500 iterations with a base of 0.96 until it reaches the minimum value of 0.0001.

A. GA vs. baseline algorithms:

We first compare two variants of GA against the three baselines to determine their effectiveness. The two versions of GA are distinguished by their exploration and exploitation policies. Figure 4a shows the performance of dynamic and static versions of GA compared to the three baselines. We constrain each user pair in each organization to use a maximum of 3 paths. We plot the aggregate weighted entanglement generation rate (W-EGR) as a function of the number of generations of the GA. The plot demonstrates that even if GA commences with a population of solutions inferior to those generated by the baselines, it eventually converges to a better solution. We observe that the dynamic version of GA converges faster as compared to the static version since the latter does not adequately explore the search space at the beginning. We will employ dynamic version of GA in later experiments.

B. GA vs. Search Space

We now investigate the impact of search space size and problem size on the convergence rate of GA and quality of the solution. In particular, we explore how the size of the search space for paths and the number of user pairs in each organization affects convergence of the GA. We hypothesize that a smaller search space will lead to faster convergence, while a larger search space will lead to slower convergence but a better solution. This pattern is indeed what we observe in Figures 4b, 4c. As the number of candidate paths increases (Figure 4b), GA is able to choose paths from a larger set, resulting in a better solution. However, it takes more generations to converge. Similarly, when the number of user pairs in each organization increases (Figure 4c) GA requires more generations to find better paths for each user pair.

C. Benefit of multiple paths in a qVPN

Now we investigate the benefits of using multiple paths in a qVPN. Figure 5 illustrates that utilizing multiple paths can offer higher rates than a single path. Moreover, using multiple paths can aid GA and the baselines in finding feasible solutions to the optimization problem. Specifically the figure shows that, when the number of paths per user pair is one, W-EGR is zero for GA, indicating that it is infeasible to satisfy the minimum rate constraint. Although our network can generate thousands of EPR pairs per second, satisfying the 10 EPRs minimum rate constraint requires a significant amount of network resources for distillation to meet the minimum fidelity threshold for each of the 10 EPR pairs. Therefore, using multiple paths can enhance the results. However, in a

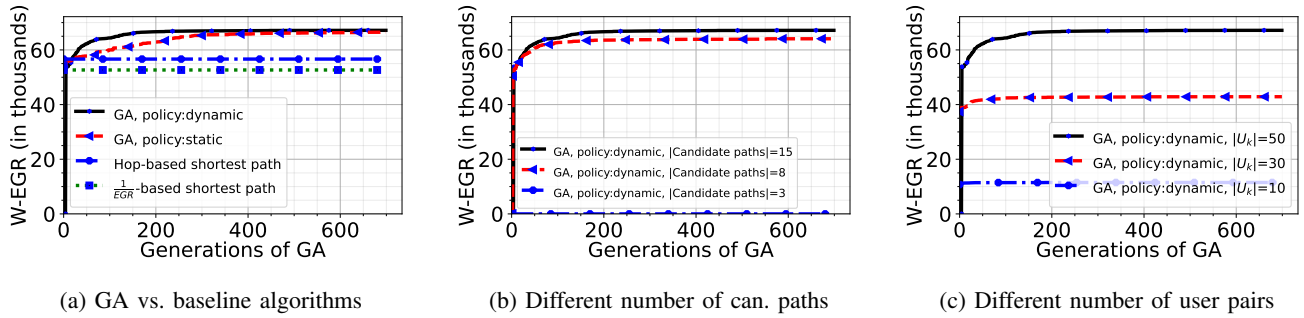


Figure 4: Evolution of GA over 1000 generations in different setups. GA over-performs the baseline algorithms (4a), explores the available paths as candidate paths successfully (4b), and is able to handle different problem sizes (4c).

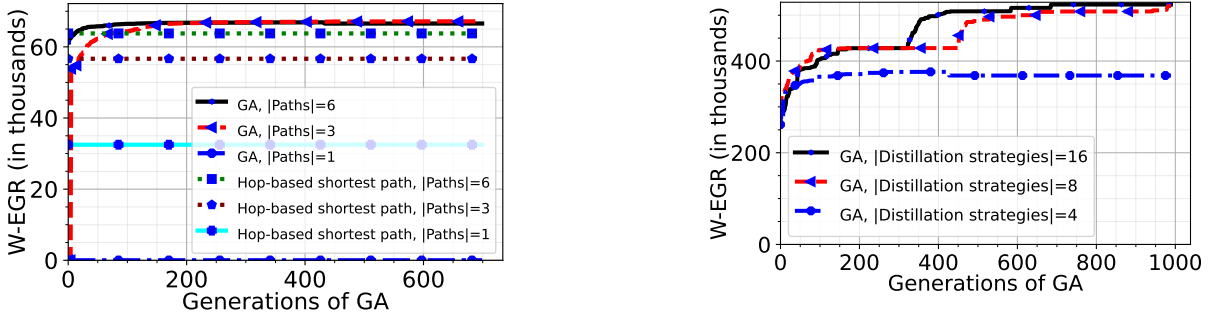


Figure 5: Effect of using multiple paths in a qVPN (zero W-EGR indicates the infeasibility of solving the optimization problem).

scenario where the set of user pairs is changing over time, and different paths need to be identified and installed for each user pair, the overhead of having multiple paths for each user pair could become a bottleneck. This scenario is similar to the problem of network updating in classical networks [16], [24], [17], which we consider as a potential area of future research.

D. Distillation strategies

This section evaluates the effectiveness of GA in selecting different distillation strategies for various paths. To test GA’s ability to handle paths of diverse lengths, user pairs are randomly selected from anywhere in the network, regardless of distance. However, it is important to note that this approach may not result in a solution that satisfies the minimum rate constraint for user pairs. To address this issue, the minimum rate constraint is set to zero and the maximum rate constraint is set to infinity. Figure 6 depicts the aggregate W-EGR across all organizations when GA has access to different numbers of distillation strategies for each path. As expected, GA can select paths with more distillation options more efficiently, resulting in increased aggregate throughput.

E. Gradient-based scheme and GA vs. baseline algorithms

We now evaluate our proposed *Gradient-based* scheme’s speed and effectiveness in selecting paths in the network

Figure 6: Effect of the number of available distillation strategies on W-EGR.

compared to GA and our baseline algorithms. For this experiment, we set up a single organization with 150 user pairs and considered only one distillation strategy (i.e., only end-level distillation) for each path. We did not set any minimum or maximum rate constraint for the user pairs, but we chose the fidelity threshold of user pairs uniformly in the range [0.85, 0.96]. For this and the next experiment setup, we have used the default version of the SURFnet network (no repeater placement) with a multiplexing value of 4 for each link. We use the k -shortest path computed using three greedy-based heuristic schemes to build our candidate paths for GA and *Gradient-based* scheme. k in this experiment similar to other sections is 5. The values of α , η , and P_2 are 0.1, 1.0 and 1.0 respectively.

Figure 7 shows the evolution of W-EGR in GA as a function of the number of generations and also the convergence of our *Gradient-based* scheme as a function of training epochs. While these two terms are different, we have plotted them together for simplicity. We see that GA and the *Gradient-based* scheme converge to almost the same solution and both over-perform the baseline algorithms. While the *Gradient-based* scheme starts with a random solution (initializing the weights of the neural network randomly VII) and so has a lower W-EGR at the beginning, it finds the best tuning for the neural network later and converges to what GA is able to. On the other hand, GA starts with a better solution as it has been initialized with our *Hop-based* shortest path heuristic. The other observation is that there is some oscillation in the

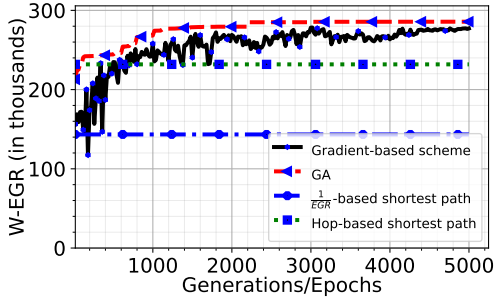


Figure 7: *Gradient-based* and GA schemes vs. baseline algorithms.

behavior of the *Gradient-based* scheme over time and we do not have this behavior in GA. The reason is that GA has the ability to save the best solution from the previous generations and always replace the current best solution with a better solution in the newly generated population. On the other hand, the current implementation of our *Gradient-based* scheme does not have this ability.

F. Processing time of GA and *Gradient-based* scheme

As a follow-up, in this experiment, we evaluate the processing time of GA and compare it with the proposed *Gradient-based* scheme. We have conducted this experiment on a Ubuntu 20.04.5 LTS the Focal Fossa version with 6 CPUs and 8 GB RAM.

Figure 8 presents the aggregate W-EGR of the user pairs as a function of the processing time of GA and the *Gradient-based* scheme in minutes. The population size for GA setup is 100. The graph shows that the *Gradient-based* scheme can find the same paths as the GA but with a significantly lower processing time. The conclusion from considering the results from figure 7 and this figure is that while the *Gradient-based* scheme needs more number of epochs to converge compared to the number of generations in GA, it has much less processing time for each epoch compared to GA processing time at each generation number. Basically, the processing for each epoch in the *Gradient-based* scheme is to solve the optimization problem 1 for all states in the batch and compute the gradients of the neural network and update its weights (more on this in section §VII). The size of the batch in the *Gradient-based* scheme is negligible compared to the population size in GA. On the other hand, GA needs to evaluate all individuals (candidate solutions) in the current population and apply genetic algorithm operations to them to generate a new population. This process is time-consuming for big population sizes. One can reduce this processing time by reducing the population size in GA. But unfortunately, GA with smaller population sizes was not able to find good solutions for the problem we have in this paper.

The downside of the *Gradient-based* scheme is that its performance is sensitive to the problem and the output size. If we consider more distillation strategies for each path, the number of outputs in Figure 3 will be enormous. In this

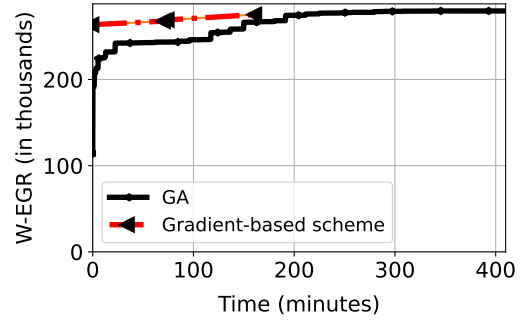


Figure 8: Convergence of genetic and *Gradient-based* algorithms.

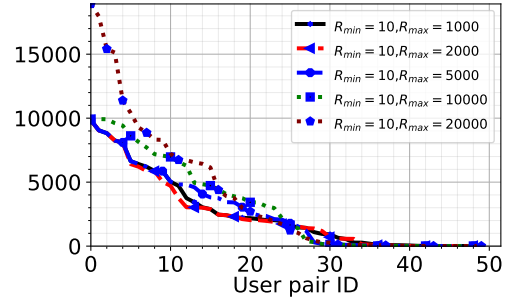


Figure 9: True rates of each user pair in one organization with different maximum rate constraints.

experiment, our neural network has three layers, and the first layer is a convolutional layer with 128 filters. When we have a setup with multiple organizations and a minimum rate constraint, finding the optimal output sizes of the neural networks becomes crucial. We leave this as a potential area of future work.

G. Fairness among user pairs

In this section, we examine the results of our qVPN in greater detail by analyzing the rates obtained by each user pair. While it may be expected that the optimization solver prioritizes user pairs with higher weights, we find that the length of the shortest paths used by each user pair and their fidelity threshold have a greater impact on the final rate that they receive from the network. To provide further insight into this, we present plots of the true EGR (unweighted) values received by each user pair under various minimum and maximum rate constraints.

In order to shape the traffic in the network, one approach is to vary the maximum rate constraints for each user pair. We set a minimum rate constraint of 10 for all user pairs in each organization and a maximum rate constraint chosen uniformly at random from $[10, R_{max}]$. We vary R_{max} and use GA to optimize for the given configuration.

Figure 9 depicts the true EGR obtained by each pair of users under different maximum rate constraints. The x -axis represents the user pairs sorted in descending order based on their true EGR. Several noteworthy observations can be made

Parameter	λ_u^k	F_u^k	L_u^k	$\frac{w_k \lambda_u^k}{F_u^k * L_u^k}$
Correlation value	0.186	-0.163	-0.636	0.576

Table III: Correlation coefficient for user pairs received true rates and their characteristics (parameters).

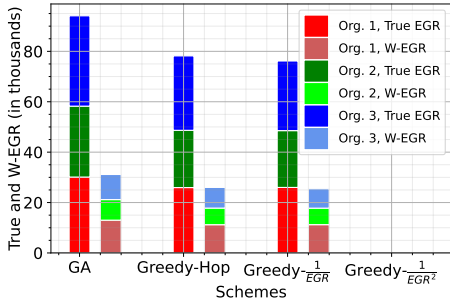


Figure 10: True and weighted rates (W-EGR) delivered to each organization in different schemes.

from Figure 9. As anticipated, decreasing the maximum rate constraint results in user pairs receiving more comparable rates from the network. However, the aggregate W-EGR decreases due to the lower maximum rate constraint.

Table III displays the correlation coefficients that describe the association between a user pair’s actual rate and the values of λ_u^k , L_u^k , F_u^k , and $\frac{w_k \lambda_u^k}{F_u^k * L_u^k}$. Here, L_u^k is the length of the shortest path used by user pair u belonging to organization k . We anticipate that user pairs with higher weights, lower fidelity thresholds, and shorter shortest path lengths will require fewer resources for distillation, making it easier to increase their EGR. The correlation coefficients reported in Table III for these metrics are consistent with this expectation. The correlation coefficient is a numerical value ranging between -1.0 and 1.0 that reflects the degree of correlation between two entities. The value of the correlation coefficient for the true EGR and both L_u^k , F_u^k are negative. This is in line with our expectation that user pairs with lower EPR fidelity requirements (lower F_u^k) would have higher rates, as fewer network resources would be allocated to distillation for those pairs. The correlation coefficient value between the true rate and $\frac{w_k \lambda_u^k}{F_u^k * L_u^k}$ is notably high and positive.

We now examine the results of our experiments to explore how the resources are distributed among various organizations in the network following the application of the GA optimization method, that maximizes the aggregate W-EGR. Figure 10 shows the true and W-EGR for each organization in different schemes. We assigned a value of zero to the true and W-EGR for the Shortest EGR-Square-based scheme, since this scheme did not yield a viable solution using the suggested paths. The resources are allocated to the user pairs of each organization based on their weight. The higher the weight of the organization, the higher the true rate for that organization. It can be observed that GA surpasses all the baseline heuristics in terms of performance at the organization level.

V. RELATED WORK

In this section, we overview the current state of research on resource management in quantum networks. While previous state-of-the-art studies [5], [25], [22], [26], [19], [3] have mainly concentrated on developing routing protocols and path selection in quantum networks, there has been limited attention given to addressing resource management challenges related to entanglement distribution among multiple end-user pairs. Authors in [8] introduce a method for optimizing the generation and distribution of entanglement through a combination of genetic algorithm and simulations of a linear quantum network. [6] addresses the problem of scheduling in the context of entanglement distribution. The authors have proposed a universal framework consisting of heuristic algorithms that prioritize minimizing application delay while also maximizing the entanglement rate and fidelity of E2E EPRs. The authors in [19] have proposed a centralized multi-path algorithm for quantum lattice networks with limited link capacities, while also ensuring a minimum E2E fidelity via only link-level purification. The proposed algorithm first identifies k shortest paths for each user pair and then assigns link-level EPRs to paths based on concepts borrowed from classical network literature, such as proportional share and progressive filling. In [30], the authors have developed entanglement distribution and purification protocols aimed at maximizing the distillable entanglement rate in a grid quantum network. For path selection, the authors propose three different strategies by assigning costs to links in the network and utilizing Dijkstra’s algorithm to identify the shortest path for each end-user pair. In [4], authors consider a set up with multiple end user pairs, and optimize the distribution rate of EPR-pairs between them using an efficient linear programming formulation subject to minimum E2E fidelity constraint. However, the authors do not consider entanglement distillation and remove the paths from the candidate set which do not meet E2E fidelity requirement. None of the above mentioned works consider a multiorganizational setting with a share public quantum network infrastructure. Moreover, little focus has been given to access the fairness of the proposed resource allocation solution among different end-user pairs.

VI. CONCLUSION AND FUTURE WORK

In this paper, we introduced qVPNs and provided a thorough analysis and evaluation of their design. While VPNs are a well-established concept in the classical setting, we present the first comprehensive design and problem formulation of qVPNs. The main contributions of this work include formulating the resource allocation problem in qVPNs and demonstrating the ability to meet user specified QoS requirements using genetic algorithm and reinforcement learning based heuristics. Going forward, we plan to examine how memory decoherence affects the performance of qVPN. Additionally, we intend to explore situations where the set of user pairs is dynamic and changing over time.

VII. APPENDIX

A. Gradient-based reinforcement learning for path selection

```

1: Randomly initialize policy network with weights  $\theta$ 
2:  $n = \{\}$ : Tracking the number of times we visit each state
3:  $v = \{\}$ : Tracking the average reward from each state
4: for each epoch do
5:   Sample  $B$  repeated states (e.g., list of user
6:   pair IDs)
7:   for  $t = 1$  to  $|B|$  do
8:     Sample an action  $a_{t,R}$  (based on policy
9:      $\pi$ ) for state  $s_t$ 
10:     $n[s_t] + 1$ 
11:    Execute action  $a_t$  and observe the
12:    reward  $r_t$  and transfer to the new state
13:     $s_t = s_{t+1}$  (this state could be a new or
14:    current list of user pair IDs.)
15:    if  $s_t \in v$ :
16:       $v[s_t] = v[s_t] + r_t$ 
17:       $b(s_t) = \frac{v[s_t]}{n[s_t]}$ 
18:    else:
19:       $v[s_t] = r_t, n[s_t] = 1$ 
20:    end
21:    for each state  $s_t$  in batch  $B$  do
22:       $\Delta\theta = \Delta\theta + \alpha(\Delta\theta \log \pi(a_{t,R}|s_t; \theta)(r_t -$ 
23:       $b(s_t)) + \beta \nabla_{\theta} H(\pi(\cdot|s_t; \theta)))$ 
24:      Update the parameters:  $\theta = \theta + \Delta\theta$ 
25:    end
26:  end

```

Algorithm 1: Gradient-based path selection algorithm

We describe our learning algorithm for path selection as follows. A state in this algorithm indicates the list of user pairs. This algorithm can be used to learn a policy that outputs different probabilities for different paths based on the list of input user pairs. We use a policy gradient method [29] to train the policy function. First, the algorithm randomly initializes all the weights θ of the policy network; (line 1). We update these parameters over T epochs. For each input state s_t (a list of user pairs) at epoch time t , the neural network selects action $a_{t,R}$ based on a policy π . Since R different paths are sampled for each input state s_t , we define a solution $a_t^R = (a_t^1, a_t^2, \dots, a_t^R)$ as a combination of R sampled actions using a stochastic policy $\pi(a_t^R|s_t)$ parameterized by θ . We execute the action and compute the reward (W-EGR). We use the state, action, and reward to update the weight of the network (lines 8-13).

For each state s_t in the batch B , we use the average reward of the state (computed at line 13) to update the weights of the neural network. In lines 16-17, we approximate a stochastic policy $\pi(a_t|s_t)$ parameterized by θ for selecting a solution a_t for a given state s_t . The approximation is as follows:

$$\pi(a_{t,R}|s_t; \theta) \approx \prod_{i=1}^R \pi(a_t^i|s_t; \theta).$$

In order to maximize the expected reward ($\mathbb{E}r_t$), we use gradient ascend using REINFORCE algorithm [29], [27] with a baseline ($b(s_t)$). For each state s_t , we use an average reward as the baseline. The policy parameter θ is updated with learning rate α as following:

$$\theta = \theta + \alpha \sum_t \nabla_{\theta} \log \pi(a_{t,R}|s_t; \theta)(r_t - b(s_t)).$$

In the above equation, for a given state s_t , we use $(r_t - b(s_t))$ to check how much better a specific solution is compared to the average solution (our baseline solution). Note that we have used α in the paper as a parameter that controls the fidelity and the rate of each link also. When $r_t > b(s_t)$, the probability of the solution $a_{t,R}$ is increased by updating policy parameters θ in the direction $\nabla_{\theta} \log \pi(a_{t,R}|s_t; \theta)$. The update step size is $\alpha(r_t - b(s_t))$. Otherwise, the solution probability is decreased. In this way, we reinforce actions that lead to better rewards. We use entropy factor $\beta = 0.1$ (strength of the entropy regularization term) in the training phase in order to ensure that the agent explores the action space adequately to discover good policies.

REFERENCES

- [1] Martín Abadi, Paul Barham, Jianmin Chen, Zhifeng Chen, Andy Davis, Jeffrey Dean, Matthieu Devin, Sanjay Ghemawat, Geoffrey Irving, Michael Isard, et al. Tensorflow: A system for large-scale machine learning. In *12th {USENIX} Symposium on Operating Systems Design and Implementation ({OSDI} 16)*, pages 265–283, 2016.
- [2] Charles H Bennett and Gilles Brassard. Quantum cryptography: Public key distribution and coin tossing. *arXiv:2003.06557*, 2020.
- [3] Marcello Caleffi. Optimal routing for quantum networks. *IEEE Access*, 5:22299–22312, 2017.
- [4] Kaushik Chakraborty, David Elkouss, Bruno Rijsman, and Stephanie Wehner. Entanglement distribution in a quantum network: A multicommodity flow-based approach. *IEEE Transactions on Quantum Engineering*, 1:1–21, 2020.
- [5] Kaushik Chakraborty, Filip Rozpedek, Axel Dahlberg, and Stephanie Wehner. Distributed routing in a quantum internet. *arXiv preprint arXiv:1907.11630*, 2019.
- [6] Claudio Ciconetti, Marco Conti, and Andrea Passarella. Request scheduling in quantum networks. *IEEE Transactions on Quantum Engineering*, 2:2–17, 2021.
- [7] J Ignacio Cirac, AK Ekert, Susana F Huelga, and Chiara Macchiavello. Distributed quantum computation over noisy channels. *Physical Review A*, 59(6):4249, 1999.
- [8] Francisco Ferreira Da Silva, Ariana Torres-Knoop, Tim Coopmans, David Maier, and Stephanie Wehner. Optimizing entanglement generation and distribution using genetic algorithms. *Quantum Science and Technology*, 6(3):035007, 2021.
- [9] G Mauro D’Ariano, Paoloplcido Lo Presti, and Matteo GA Paris. Using entanglement improves the precision of quantum measurements. *Physical review letters*, 87(27):270404, 2001.
- [10] David Deutsch, Artur Ekert, Richard Jozsa, Chiara Macchiavello, Sandu Popescu, and Anna Sanpera. Quantum privacy amplification and the security of quantum cryptography over noisy channels. *Phys. Rev. Lett.*, 77:2818–2821, Sep 1996.
- [11] N. G. Duffield, Pawan Goyal, Albert Greenberg, Partho Mishra, K. K. Ramakrishnan, and Jacobus E. van der Merive. A flexible model for resource management in virtual private networks. SIGCOMM ’99, page 95–108. Association for Computing Machinery, 1999.
- [12] Wolfgang Dür, H-J Briegel, Juan Ignacio Cirac, and Peter Zoller. Quantum repeaters based on entanglement purification. *Physical Review A*, 59(1):169, 1999.

- [13] Anupam Gupta, Jon Kleinberg, Amit Kumar, Rajeev Rastogi, and Bulent Yener. Provisioning a virtual private network: A network design problem for multicommodity flow. In *Proceedings of the Thirty-Third Annual ACM Symposium on Theory of Computing*, STOC '01, page 389–398. Association for Computing Machinery, 2001.
- [14] Peter C Humphreys, Norbert Kalb, Jaco PJ Morits, Raymond N Schouten, Raymond FL Vermeulen, Daniel J Twitchen, Matthew Markham, and Ronald Hanson. Deterministic delivery of remote entanglement on a quantum network. *Nature*, 558(7709):268–273, 2018.
- [15] IBM. IBM [Online]. <https://www.ibm.com/academic>, 2022. [Online; accessed 2-Jun-2022].
- [16] Xin Jin, Hongqiang Harry Liu, Rohan Gandhi, Srikanth Kandula, Ratul Mahajan, Ming Zhang, Jennifer Rexford, and Roger Wattenhofer. Dynamic scheduling of network updates. *ACM SIGCOMM Computer Communication Review*, 44(4):539–550, 2014.
- [17] H. Kim, J. Reich, A. Gupta, M. Shahbaz, N. Feamster, and R. Clark. Kinetic: Verifiable dynamic network control. In *NSDI 15*, 2015.
- [18] Peter Komar, Eric M Kessler, Michael Bishof, Liang Jiang, Anders S Sørensen, Jun Ye, and Mikhail D Lukin. A quantum network of clocks. *Nature Physics*, 10(8):582–587, 2014.
- [19] Changhao Li, Tianyi Li, Yi-Xiang Liu, and P. Cappellaro. Effective routing design for remote entanglement generation on quantum networks. *npj Quantum Information*, 7(10), 2021.
- [20] Sreraman Muralidharan, Linshu Li, Jungsang Kim, Norbert Lütkenhaus, Mikhail D Lukin, and Liang Jiang. Optimal architectures for long distance quantum communication. *Scientific reports*, 6(1):20463, 2016.
- [21] University of Adelaide. The Internet Topology Zoo [Online]. <http://www.topology-zoo.org/dataset.html>, 2023. [Online; accessed 2-January-2023].
- [22] Mihir Pant, Hari Krovi, Don Towsley, Leandros Tassioulas, Liang Jiang, Prithwish Basu, Dirk Englund, and Saikat Guha. Routing entanglement in the quantum internet. *npj Quantum Information*, 5(1):1–9, 2019.
- [23] Momtchil Peev, Christoph Pacher, Romain Alléaume, Claudio Barreiro, Jan Bouda, W Boxleitner, Thierry Debuisschert, Eleni Diamanti, Mehrdad Dianati, JF Dynes, et al. The secoqc quantum key distribution network in vienna. *New Journal of Physics*, 11(7):075001, 2009.
- [24] Mark Reitblatt, Nate Foster, Jennifer Rexford, Cole Schlesinger, and David Walker. Abstractions for network update. *ACM SIGCOMM Computer Communication Review*, 42(4):323–334, 2012.
- [25] Eddie Schoute, Laura Mancinska, Tanvirul Islam, Iordanis Kerenidis, and Stephanie Wehner. Shortcuts to quantum network routing. *arXiv preprint arXiv:1610.05238*, 2016.
- [26] Shouqian Shi and Chen Qian. Concurrent entanglement routing for quantum networks: Model and designs. In *Proceedings of the Annual conference of the ACM Special Interest Group on Data Communication on the applications, technologies, architectures, and protocols for computer communication*, pages 62–75, 2020.
- [27] D. Silver, G. Lever, N. Heess, T. Degris, D. Wierstra, and M. Riedmiller. Deterministic policy gradient algorithms. In *International conference on machine learning*, pages 387–395. PMLR, 2014.
- [28] Damien Stucki, Matthieu Legre, Francois Buntschu, B Clausen, Nadine Felber, Nicolas Gisin, Luca Henzen, Pascal Junod, Gérald Litzistorf, Patrick Monbaron, et al. Long-term performance of the swissquantum quantum key distribution network in a field environment. *New Journal of Physics*, 13(12):123001, 2011.
- [29] Richard S Sutton, David McAllester, Satinder Singh, and Yishay Mansour. Policy gradient methods for reinforcement learning with function approximation. *Advances in neural information processing systems*, 12:1057–1063, 1999.
- [30] Michelle Vitoria, Stefan Krastanov, Alexander Sanchez de la Cerda, Steven Willis, and Prineha Narang. Purification and entanglement routing on quantum networks. *arXiv preprint arXiv:2011.11644*, 2020.
- [31] Shuang Wang, Wei Chen, Zhen-Qiang Yin, Hong-Wei Li, De-Yong He, Yu-Hu Li, Zheng Zhou, Xiao-Tian Song, Fang-Yi Li, Dong Wang, et al. Field and long-term demonstration of a wide area quantum key distribution network. *Optics express*, 22(18):21739–21756, 2014.
- [32] Jin Y Yen. Finding the k shortest loopless paths in a network. *management Science*, 17(11):712–716, 1971.